



Nonlinear and linear analysis of Direct Yellow 50 adsorption onto modified graphene oxide: kinetic, isotherm, and thermodynamic studies

Avideh Azizi^a, Elham Moniri^{b,*}, Amir Hessam Hassani^a, Homayon Ahmad Panahi^c, Mohamadreza Jafarinezhad^d

^aFaculty of Natural Resources and Environment, Science and Research Branch, Department of Environmental Engineering, Islamic Azad University, Tehran, Iran, emails: avideh_85@yahoo.com (A. Azizi), ahhassani@srbiau.ac.ir (A.H. Hassani)

^bDepartment of Chemistry, Varamin (Pishva) Branch, Islamic Azad University, Pishva, Iran, Mobile No. 0098-91-2501-1003; email: moniri30003000@yahoo.com

^cDepartment of Chemistry, Central Tehran Branch, Islamic Azad University, Tehran, Iran, email: h.ahmadpanahi@iauctb.ac.ir

^dFaculty of Engineering, Department of Mechanical Engineering, South Tehran Branch, Islamic Azad University, Tehran, Iran, email: m.r.jafarinezhad@gmail.com

Received 4 December 2020; Accepted 24 April 2021

ABSTRACT

The present work describes the removal of Direct Yellow 50 from an aqueous solution by graphene oxide modified with 4-aminodiphenylamine (GO-A). The final adsorbent was characterized by carbon, hydrogen, and nitrogen analysis, Brunauer–Emmett–Teller technique, Fourier transform-infrared resonance spectroscopy, and scanning electron microscopy. Batch studies were carried out to investigate the effect of experimental factors such as contact time (5–120 min), initial dye concentration (10–80 mg/L), and temperature (25°C, 35°C, and 45°C) on the GO-A adsorption of dye. The linear and non-linear forms of kinetic and isotherm models were also investigated. The isotherm and kinetic data of dye were correlated reasonably well by non-linear Freundlich and Elovich models, respectively. The thermodynamic studies showed that the dye adsorption onto GO-A is a spontaneous, favorable, and exothermic process. Additionally, dye isotherm studies revealed that maximum dye adsorption capacities of 10.71, 8.03, and 5.71 mg/g were achieved for 25°C, 35°C, and 45°C temperatures, respectively. It can be collected that GO-A could be applied as an effective adsorbent for the removal of dye.

Keywords: Adsorption; Direct Yellow 50; Graphene oxide; Non-linear; Thermodynamic; Isotherm; Kinetic

1. Introduction

Dyes emitted from textile, rubber, paper, and dye manufacturing to the aqueous environment are toxic compounds. Pigments and dyes have serious threats such as carcinogenic, mutagenic, and teratogenic hazards for humans, animals, and other living organisms in the environment [1]. A variety of dyes, including anionic (direct, reactive, and acid dyes), cationic (basic dyes), and non-ionic (disperse dyes), are utilized in industrial dyeing processes

[2]. Direct Yellow 50, as an anionic dye, has the highest value of solubilization capacity [1]. This dye is frequently used in the dye industry, hence, it is necessary to remove the Direct Yellow 50 from wastewaters due to its toxic nature and high solubility. Currently, many procedures have been applied to remove the dyes from the aqueous solution, which include coagulation, chemical oxidation, flocculation, adsorption, and advanced oxidation processes [3]. The adsorption technique has been found to be superior due to reasons such as its low cost, high efficiency, easy

* Corresponding author.

design, simple operation, without creation of sludge, low energy requirement, available adsorbents, and biodegradability [2,4,5].

To date, a vast diversity of adsorbents has been tested for the removal of dyes from wastewater, including activated carbon, graphene oxide (GO), clay, zeolites, alumina, fly-ash, and silica [5–8]. Among these, GO has been indicated to be an efficient adsorbent for the removal of pollutants from wastewater [7]. Graphene is an allotrope of carbon including the flat single sheet of graphite with sp^2 -bonded carbon atoms [5]. GO is the graphene derivative that contains oxygen functional groups (carboxyl, hydroxyl, and epoxy groups) [9]. These functional groups improve interactions with organic dyes [10]. Moreover, the reactive oxygen groups increase the potential of modification for the GO surface [10]. In recent years, GO has received wide interest as an adsorbent because of its environmentally friendly nature, chemical stability, and cost-effectiveness [11,12]. Practically, GO interactions are based on the hydrogen bonding, electrostatic interaction, and π - π binding [13]. Researchers also reported that graphene-based materials could be easily regenerated several times with no significant changes in their adsorption capacity [14].

Therefore, in this paper, modified graphene oxide was prepared using 4-aminodiphenylamine as an adsorbent to remove Direct Yellow 50 from aqueous solutions. Effective parameters such as contact time, dye concentration, and temperature were examined on dye adsorption. The experimental data were investigated via the pseudo-first-order, pseudo-second-order, intraparticle diffusion, and Elovich kinetic models. Langmuir, Freundlich, Dubinin–Radushkevich, and Temkin models were used to fit the equilibrium data. The thermodynamic parameters and activation energy of dye adsorption were also assessed. The linear and non-linear isotherm, kinetic, and thermodynamic studies were applied to estimate the adsorption capacity of GO-A.

2. Experimental

2.1. Materials

4-aminodiphenylamine (purity $\geq 98\%$), cyanuric chloride (purity $\geq 99\%$), graphite powder ($<50 \mu\text{m}$, purity $\geq 99.5\%$), KMnO_4 , NaNO_3 , H_2SO_4 (95%–97%), H_2O_2 (30%), HCl (37%), sodium acetate trihydrate, sodium chloride, acetic acid (100%), and methanol (purity $\geq 99.5\%$) were procured from Merck (Germany). Direct Yellow 50 and petroleum were obtained from Sigma-Aldrich Company and Romil pure chemistry, respectively. All chemicals used were of analytical grade.

2.2. Synthesis of modified graphene oxide

The Hummers and Offeman method was applied in the synthesis of GO [15]. At first, the graphite powder (10 g), NaNO_3 (5 g), and H_2SO_4 (230 mL) were mixed for 1 h at room temperature under stirring. Afterwards, 30 g of KMnO_4 were moderately added into the solution. The mixture was poured into an ice bath with constant stirring for 2 h. Then, 460 mL of distilled water was gradually added

to the mixture. Finally, 325 mL of H_2O_2 (30%) was added to stop the reaction and remove the residual metal ions. The mixture was heated between 90°C and 100°C , and kept stirred for 2 h. The resulting product was washed with HCl (3%) and distilled water several times until reaching pH 7, followed by filtration and drying at 45°C for 2 d in an oven. The GO was characterized with different techniques such as carbon, hydrogen, and nitrogen analysis (CHN; Eager 300 for 1112, USA), Brunauer–Emmett–Teller (BET; BELSORP-mini II, Japan), Fourier transform–infrared resonance (FT–IR; Thermo Nicolet, model: NEXUS 870 FT–IR, USA), and scanning electron microscopy (SEM; Zeiss, model: Sigma, Germany) analysis.

GO-A was prepared using the suggested process by Azizi et al. [5]. At first, 1 g of GO was dissolved in 40 mL of petroleum ether and stirred for 1 h. The solution was then ultra-sonicated for 30 min using an ultrasonic cleaner (WUC-A03H, Korea). Cyanuric chloride (1 g) was added to the mixture and the sample was agitated in a rotary shaker (IKA, KS 260 Basic, Korea) with 100 rpm for 10 h. After remaining in the same condition for 24 h, the suspension was washed with petroleum ether (25 mL). Finally, the product was stirred for 24 h and dried in an oven.

At the end of the procedure, 4-aminodiphenylamine (0.5 g) was dissolved in methanol and acetate sodium buffer solution (pH 5, 0.01 M) under stirring at room temperature. Grafted GO with cyanuric chloride was added to the mixture and shaken at 70°C – 80°C for 2 d. At last, the sample was washed with sodium chloride, acetate sodium buffer, distilled water, and methanol, respectively. After filtering, the final product was dried at 40°C for 2 d. GO-A was characterized by CHN, BET, FT–IR, and SEM techniques.

2.3. Adsorption experiments

A batch sorption experiment was carried out for the removal of Direct Yellow 50 via GO-A. The samples were placed into the rotary shaker (IKA, KS 260 Basic, Korea) at 150 rpm. Then, the solutions were filtered with a syringe filter ($0.22 \mu\text{m}$ pore size). The concentration of Direct Yellow 50 was determined by using a HACH spectrophotometer (DR/5000) at $\lambda_{\text{max}} = 396 \text{ nm}$. The amount of dye removal efficiency (RE) and adsorbed dye (q_t , mg/g) were evaluated in the following:

$$\text{RE}(\%) = \frac{C_0 - C_t}{C_0} \times 100 \quad (1)$$

$$q_t = \frac{(C_0 - C_t)v}{m} \quad (2)$$

where C_0 and C_t represent the initial and the t -time concentration of Direct Yellow 50 (mg/L), respectively, v and m are the volume of dye solution (L) and the mass of GO-A (g), respectively.

2.4. Kinetic modeling

Kinetic experiments were carried out under the following conditions: initial dye concentration = 20 mg/L,

adsorption dose = 1 g/L, pH = 7, agitation speed = 150 rpm, at different temperatures (25°C, 35°C and 45°C), and a range of 5–120 min for contact time. Different models can be applied to explain the mechanism of solute sorption onto a sorbent. The sorption kinetics of the dye was investigated using the pseudo-first-order [7,16], pseudo-second-order [7,16], intraparticle diffusion, [17] and Elovich models [17,18]. Linear and non-linear kinetic equations of adsorption are presented in Table 1.

The activation energy of dye adsorption (E_a) onto the adsorbent can be obtained by the following Arrhenius type relationship:

$$k_2 = A \exp\left(-\frac{E_a}{RT}\right) \quad (3)$$

where k_2 and A are the pseudo-second-order constant (g/mg min) and the Arrhenius factor, respectively. E_a (J/mol) is the activation energy of adsorption and T is the solution temperature (K).

2.5. Adsorption isotherms

The isotherm of dye adsorption on GO-A was studied at the contact time of 90 min, adsorption dose of 1 g/L, pH of 7, agitation speed of 150 rpm, at different temperatures (25°C, 35°C and 45°C), and the range of 10–80 mg/L for initial dye concentration. Adsorption isotherms present the interaction between the adsorbent materials and contamination. Langmuir, Freundlich, Dubinin–Radushkevich, and Temkin equations were tested in this work. In Langmuir isotherm model, the adsorption occurs in monolayers at homogeneous sites on the adsorbent [5,16]. The Freundlich isotherm is for the sorption on a heterogeneous surface and reversible adsorption [16,19]. The isotherm of Dubinin–Radushkevich is used to estimate the chemical or physical mechanism [5,17,20]. Temkin isotherm describes the heat of adsorption and the adsorbent–adsorbate interaction [21,22]. The linear

and non-linear equations of isotherm have been given in Table 2.

2.6. Error functions

The error analysis was estimated to predict best-fitting kinetic and isotherm models. Therefore, in this study, the chi-square function (χ^2) was calculated to determine the better kinetic and isotherm equation between linear and non-linear models. The χ^2 equation can be expressed as [23]:

The best fit model was evaluated by the minimum level of χ^2 .

$$\chi^2 = \sum_{i=1}^p \frac{(q_e - q_{cal})^2}{q_e} \quad (4)$$

2.7. Adsorption thermodynamics

To evaluate the effect of temperature on the adsorption of Direct Yellow 50 onto GO-A, the non-linear thermodynamic parameters were determined. The changes in free energy (ΔG° , kJ/mol), enthalpy (ΔH° , kJ/mol), and entropy (ΔS° , kJ/mol K) of the biosorption process were obtained using the following equations:

$$K_l = \exp\left(\frac{\Delta S^\circ}{R} - \frac{\Delta H^\circ}{RT}\right) \quad (5)$$

$$K_l = \exp\left(\frac{-\Delta G^\circ}{RT}\right) \quad (6)$$

$$\Delta G^\circ = \Delta H^\circ - T\Delta S^\circ \quad (7)$$

where K_l is the equilibrium constant (acquired from the Langmuir model), R is the gas constant (8.314 J/mol K), and T is the absolute temperature (K).

Table 1
List of adsorption kinetic models

Kinetic name	Linear	Non-linear	Parameters
Pseudo-first-order	$\log(q_e - q_t) = \log q_e - \frac{k_1}{2.303}t$	$q_t = q_e(1 - \exp(-k_1t))$	q_t = Adsorbent capacity of adsorbate at t time (mg/g) q_e = Adsorption capacity of the adsorbent at equilibrium (mg/g) k_1 = Rate constant of pseudo-first-order adsorption (1/min)
Pseudo-second-order	$\frac{t}{q_t} = \frac{1}{q_e^2 k_2} + \frac{t}{q_e}$	$q_t = \frac{q_e^2 k_2 t}{1 + q_e k_2 t}$	q_e = Adsorption capacity of the adsorbent at equilibrium (mg/g) k_2 = Rate constant of pseudo-second-order adsorption (g/mg min)
Intraparticle diffusion	–	$q_t = k_p t^{0.5} + c$	k_p = Rate constant of the intraparticle diffusion kinetic model (mg/g min ^{1/2}) c = A constant
Elovich	$q_t = \frac{1}{b} \ln(ab) + \frac{1}{b} \ln t$	$q_t = \frac{1}{b} \ln(1 + abt)$	a = The initial adsorption rate (mg/g min) b = The desorption constant (g/mg)

Table 2
List of isotherm equations

Isotherm name	Linear	Non-linear	Parameters
			C_e = Concentration of adsorbate at equilibrium (mg/L) q_e = Adsorption capacity of the adsorbent at equilibrium (mg/g)
Langmuir	$\frac{C_e}{q_e} = \frac{1}{k_1 Q_m} + \frac{C_e}{Q_m}$	$q_e = Q_m \frac{k_1 C_e}{1 + k_1 C_e}$	k_1 = Langmuir constant (L/mg) Q_m = The maximum adsorption capacity (mg/g)
Freundlich	$\log q_e = \log k_f + \frac{1}{n} \log C_e$	$q_e = k_f C_e^{1/n}$	k_f = Freundlich constant (L/mg) n = A constant related the intensity of adsorption
Dubinin–Radushkevich	$\ln q_e = \ln q_m - B\epsilon^2$ $\epsilon = RT \ln \left(1 + \frac{1}{C_e} \right)$ $E = \frac{1}{\sqrt{2B}}$	$q_e = q_m \exp(-B\epsilon^2)$	q_m = Theoretical monolayer saturation capacity (mg/g) B = Constant of the sorption energy (mol ² /kJ ²) ϵ = Polanyi potential R = Universal gas constant (8.314 J/mol K) T = Absolute temperature E = The adsorption energy (kJ/mol)
Temkin	$q_e = B_1 \ln k_t + B_1 \ln C_e$	$q_e = B_1 \ln(k_t C_e)$	B_1 = A constant related to the heat of adsorption k_t = The constant of equilibrium binding (L/mg)

Thermodynamic experiments have been performed for Direct Yellow 50 adsorptions by GO-A at different temperatures (25°C, 35°C and 45°C) under the following experimental conditions: initial Direct Yellow 50 dye concentration varies from 10 to 80 mg/L; the adsorbent dose of 1 g/L; pH of 7; agitation speed of 150 rpm; contact time of 90 min.

3. Results and discussion

3.1. Physicochemical characterization

From the CHN elemental analysis outcomes, the chemical composition of GO and GO-A are as follows (%): C: 54.69, H: 2.46, N: 0.15 for GO, C: 63.07, H: 1.59, N: 2.83 for GO-A [5]. The percentage of carbon and nitrogen was increased with the grafting GO to 4-aminodiphenylamine. The results indicated that the GO was successfully modified with 4-aminodiphenylamine.

Nitrogen adsorption and desorption isotherms were measured using a BELSORP instrument at 77 K. The total surface areas of GO and GO-A were evaluated by the BET method. Moreover, the average pore diameter and total pore volume were determined using the Barrett–Joyner–Halenda (BJH) theory. The analysis of BET revealed the same surface area for GO (13.24 m²/g) and GO-A (12.41 m²/g), approximately, while the average pore diameter and total pore volume of GO were improved from 4.853 nm and 0.016 cm³/g to 42.879 nm and 0.133 cm³/g after modification, respectively [5]. It was observed that the average pore diameter and total pore volume increased significantly according to the functional groups grafted to GO which led to relatively more empty spaces around the adsorbent [24]. There was negligible change in the surface area of the adsorbent after the modification process. This result may be due to the relative similarity of GO and GO-A structures.

The IR absorption spectra of the GO and GO-A are shown in Fig. 1. The spectrum of GO showed the bands around 1,054 and 1,222 cm⁻¹ can be assigned to the C–O bonds [5]. Peaks discovered at 1,421, 1,720, and 2,922 cm⁻¹ were due to CH₂, C=O and the aliphatic C–H groups [5]. The broad adsorption peaks at 1,628 and 3,440 cm⁻¹ were associated to the O–H group [25,26]. The FT–IR spectrum for GO-A was different than GO due to the peaks such as: C=N bonds at 1,492 and 1,578 cm⁻¹ [27,28], C=O groups at 1,718 cm⁻¹ [29]. Finally, the absorption band at 3,402 cm⁻¹ indicated the O–H and N–H stretch vibrations [24].

The surface morphologies of GO and GO-A were studied using SEM (Fig. 2). It can be noticed that the structure of GO includes many layers with the folds (Fig. 2a). Meanwhile, wrinkles were observed on the GO surface, which explained the flexibility of adsorbent. The porous structure of GO-A is seen as a layered structure in Fig. 2b, confirming the successful formation of the final adsorbent.

The mechanism for the adsorption of Direct Yellow 50 by GO-A can be assumed to involve physical adsorption. Dye diffuses into the inner pore system on the adsorbent surface active sites. Moreover, the hydrogen bond strength and π - π stacking interaction between benzene rings in the Direct Yellow 50 and rings on GO-A can be effective as the adsorption mechanism. Fig. 3 describes the adsorption mechanism of Direct Yellow 50 using GO-A.

3.2. Kinetic studies

The results of the adsorption kinetics of dye on the adsorbent at different temperatures are shown in Fig. 4.

The removal efficiency of dye increased with time and reached the equilibrium time (90 min). This enhancement of adsorption can be attributed to the available active

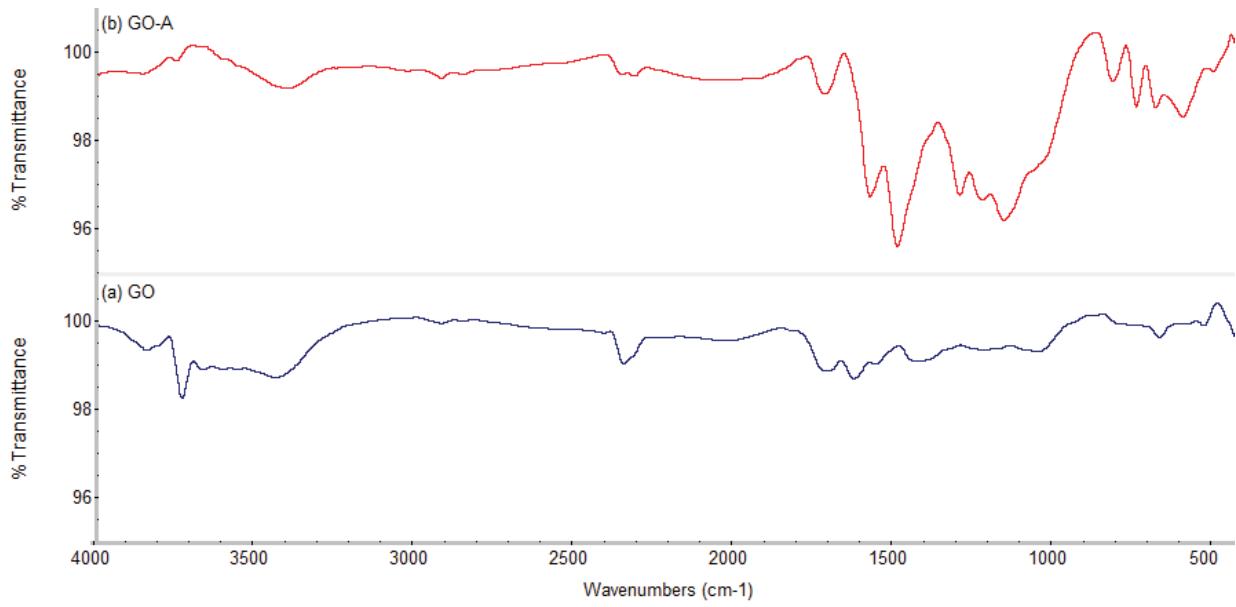


Fig. 1. FT-IR spectra of GO (a) and GO-A (b).

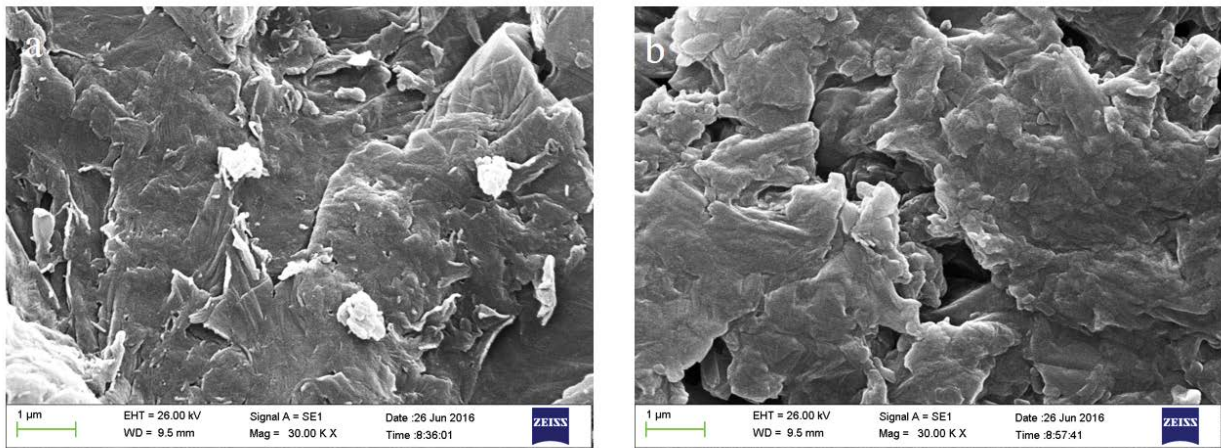


Fig. 2. SEM images of adsorbents (a) GO and (b) GO-A.

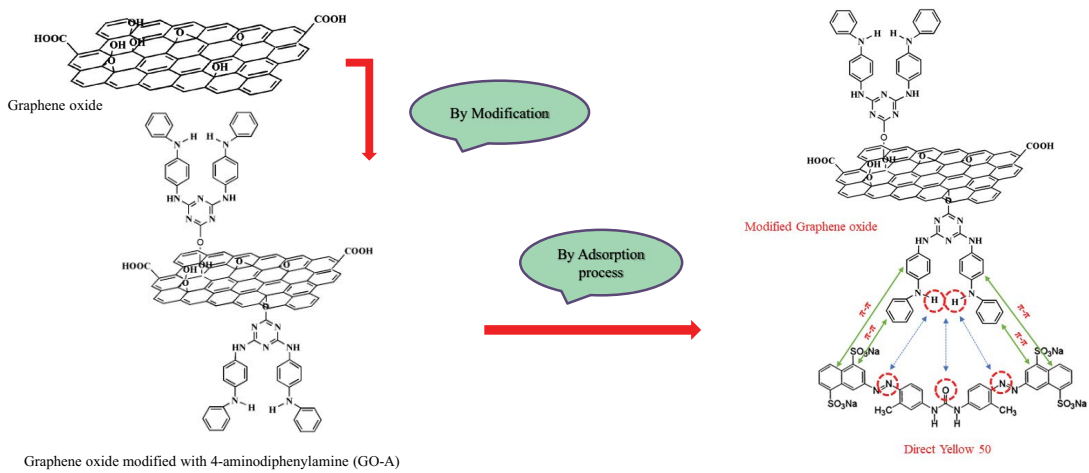


Fig. 3. The adsorption mechanism of Direct Yellow 50 using GO-A.

sites on GO-A [5]. This is in agreement with the reports of researchers [30,31]. The removal efficiency decreases with the increasing temperature, indicating the adsorption of GO-A for Direct Yellow 50 which may be an exothermic process.

The results of linear and non-linear kinetic modeling were adjusted by the pseudo-first-order, pseudo-second-order, intraparticle diffusion, and Elovich kinetic models (Table 3). The non-linear Elovich model was approved to express the process because it had a lower error level and higher R^2 . According to Table 3, the q_e values for pseudo-second-order were close to the experimental values at various temperatures. Non-linear form of kinetic models for adsorption of Direct Yellow 50 by GO-A at different temperatures is shown in Fig. 5.

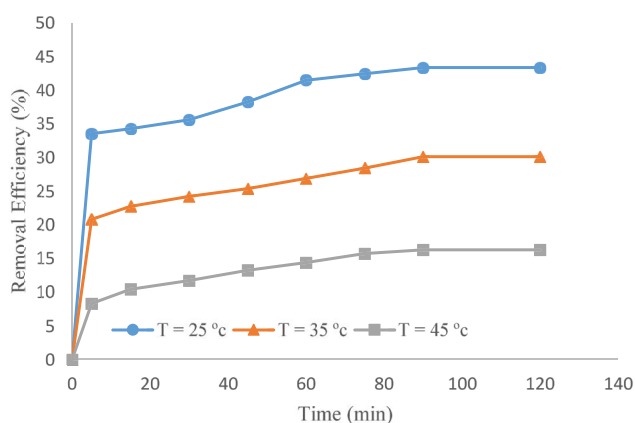


Fig. 4. Effect of contact time on removal efficiency of Direct Yellow 50 onto GO-A at different temperatures.

The values of E_a ranges from 5 to 40 kJ/mol suggest a physical adsorption, whereas the higher activation energies (40–800 kJ/mol) are related to chemical biosorption [32]. The result obtained is 17.28 kJ/mol for the dye adsorption onto GO-A adsorbent, indicating that the adsorption process is physical adsorption.

3.3. Isotherm studies

The effect of initial dye concentration on the removal efficiency by GO-A adsorbent at different temperatures is shown in Fig. 6. It was observed that the removal efficiency of Direct Yellow 50 was decreased with increasing the initial dye concentration at all temperatures. The number ratio of the dye molecules to the available adsorption sites increases at higher concentrations, which decreases the removal efficiency of dye [22]. Similar results have been reported where the removal efficiency of Direct Yellow decreased during higher concentrations using activated carbon adsorbents [1,33].

In the current study, the batch experimental data were analyzed using Langmuir, Freundlich, Dubinin–Radushkevich, and Temkin isotherms. The parameters of linear and non-linear isotherm models were listed in Table 4.

It showed the four models equilibrium adsorption of dye molecules onto the GO-A at different temperatures. As can be seen, the non-linear Freundlich model is the best-fitted model concerning not only the lowest error values, but also the highest R^2 . For non-linear Langmuir isotherm, the adsorption capacity was found to be 10.71, 8.03, and 5.71 mg/g at 25°C, 35°C, and 45°C temperatures, respectively. Based on the Freundlich analysis, $1/n$ values show the shape of isotherm to be irreversible ($1/n = 0$), favorable

Table 3 Kinetic parameters for the adsorption of Direct Yellow 50 onto GO-A

	25°C		35°C		45°C		
	Linear	Non-linear	Linear	Non-linear	Linear	Non-linear	
$q_{e(\text{exp})}$ (mg/g)	8.67		6.02		3.25		
Pseudo-first-order	$q_{e(\text{cal})}$ (mg/g)	3.18	7.98	2.21	5.40	2.20	2.97
	k_1 (1/min)	0.034	0.351	0.022	0.271	0.034	0.097
	R^2	0.907	0.943	0.955	0.931	0.920	0.907
	χ^2	19.741	0.539	11.565	0.482	1.282	0.577
Pseudo-second-order	$q_{e(\text{cal})}$ (mg/g)	9.02	8.35	6.28	5.73	3.54	3.30
	k_2 (g/mg min)	0.021	0.070	0.0230	0.070	0.025	0.041
	R^2	0.997	0.966	0.994	0.964	0.992	0.961
	χ^2	0.828	0.264	0.631	0.190	0.241	0.152
Intraparticle diffusion	k_p (mg/g min ^{1/2})		0.629		0.448		0.275
	C		3.089		1.894		0.678
	R^2		0.684		0.746		0.889
	χ^2		1.279		0.736		0.218
Elovich	a (mg/g min)	848.469	844.776	73.390	72.675	1.856	1.659
	b (g/mg)	1.371	1.370	1.615	1.612	1.834	1.786
	R^2	0.860	0.988	0.92	0.990	0.962	0.990
	χ^2	0.0923	0.092	0.050	0.050	0.037	0.040

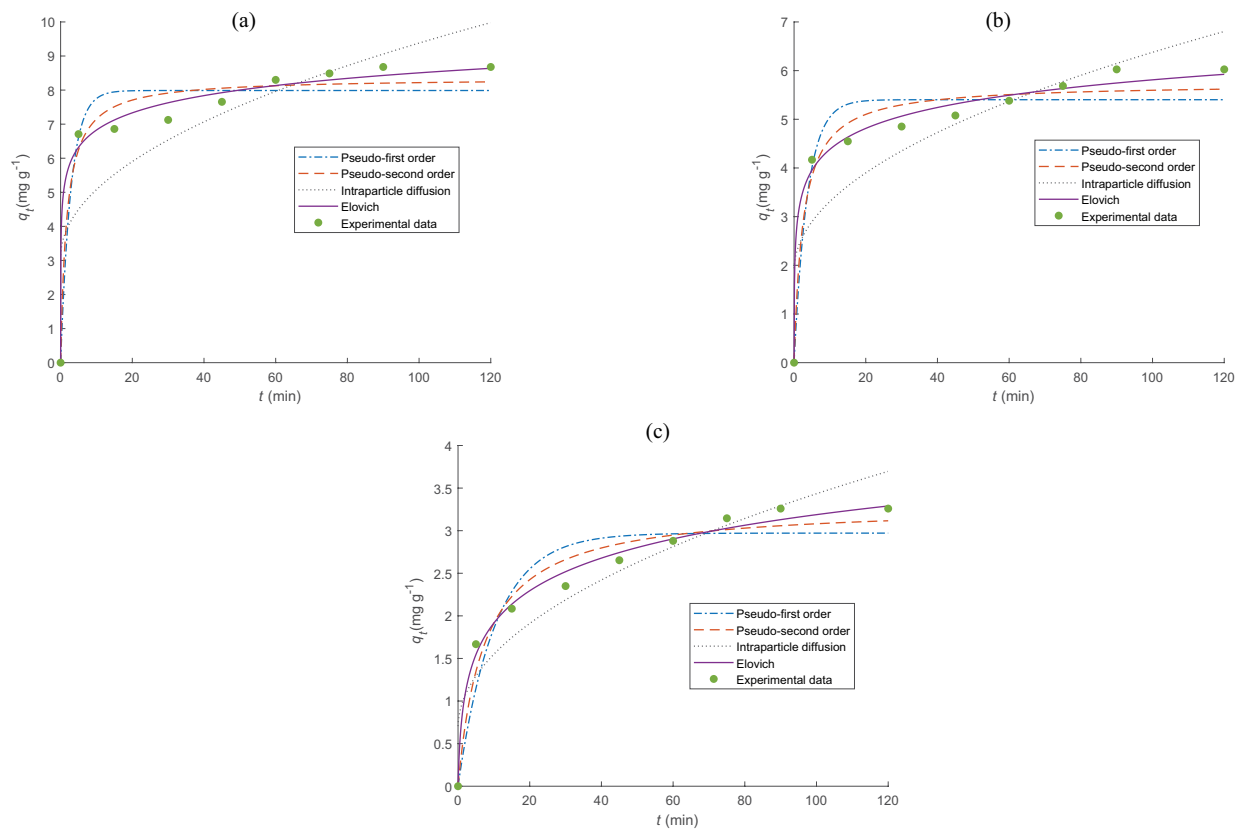


Fig. 5. Non-linear form of kinetic models for adsorption of Direct yellow 50 by GO-A at (a) 25°C, (b) 35°C, and (c) 45°C.

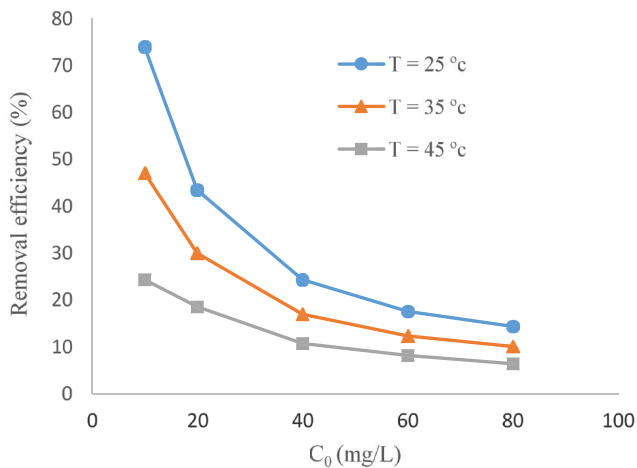


Fig. 6. Effect of initial dye concentration on removal efficiency of Direct Yellow 50 onto GO-A at different temperatures.

($0 < 1/n < 1$), unfavorable ($1/n > 1$) [34]. The results indicated that the adsorption of Direct Yellow 50 onto GO-A was favorable. The adsorption energy (E) is used to estimate the sorption mechanism as chemical ($E > 16$ kJ/mol), physical sorption ($E < 8$ kJ/mol) or, ion exchange mechanism ($8 < E < 16$ kJ/mol). The adsorption energy obtained from Dubinin–Radushkevich isotherm was in the range of $E < 8$ kJ/mol suggesting that the adsorption of dye onto

GO-A was a physical process. In addition, the non-linear curves of isotherm models are demonstrated in Fig. 7.

The maximum adsorption capacity of GO-A for Direct Yellow 50 removal was obtained 10.71 mg/g at adsorbent dose of 1 g/L, contact time of 90 min and pH of 7. Table 5 demonstrates the adsorption capacity of GO-A for Direct Yellow 50 adsorption compared with different adsorbents reported previously.

3.4. Thermodynamic studies

The effect of temperature is another important parameter because the adsorption efficiency and capacity can change when the temperature increases or decreases. The values of ΔS° and ΔH° are gained from plotting K_f against T (Fig. 8).

Table 6 shows the obtained non-linear thermodynamic parameter values. The negative values of ΔS° and ΔH° indicate that the dye adsorption process is a favorable and exothermic process, respectively [39]. Furthermore, it can be observed that ΔG° values are negative, thus reflecting the feasibility and spontaneous nature of the adsorption of Direct Yellow 50 onto GO-A.

4. Conclusions

This study reports on the possibility of using graphene oxide modified with 4-aminodiphenylamine as adsorbent

Table 4
Isotherm parameters for the adsorption of Direct Yellow 50 onto GO-A

Isotherm	Parameters	25°C		35°C		45°C	
		Linear	Non-linear	Linear	Non-linear	Linear	Non-linear
Langmuir	Q_m (mg/g)	11.68	10.71	8.46	8.03	5.77	5.71
	K_l (L/mg)	0.273	0.729	0.167	0.238	0.096	0.101
	R^2	0.993	0.975	0.994	0.990	0.997	0.996
	χ^2	0.942	0.215	0.148	0.061	0.019	0.018
	k_f (L/mg)	6.446	6.364	3.449	3.472	1.398	1.531
Freundlich	n	7.812	7.566	5.107	5.158	3.218	3.503
	R^2	0.980	0.997	0.988	0.998	0.942	0.987
	χ^2	0.022	0.023	0.011	0.011	0.069	0.071
	q_m (mg/g)	10.75	10.19	7.59	7.25	4.93	4.78
Dubinin-Radushkevich	B (mol ² /kJ ²)	5.152	0.528	8.618	2.616	13.829	7.958
	E (kJ/mol)	0.311	0.973	0.240	0.437	0.190	0.250
	R^2	0.771	0.958	0.801	0.966	0.852	0.978
	χ^2	6.715	0.362	2.124	0.205	0.369	0.182
	k_i (L/mg)	175.731	175.774	9.185	9.185	1.294	1.294
Temkin	B_1	1.171	1.171	1.211	1.211	1.133	1.133
	R^2	0.959	0.959	0.988	0.988	0.975	0.975
	χ^2	0.402	0.402	0.177	0.177	0.107	0.107

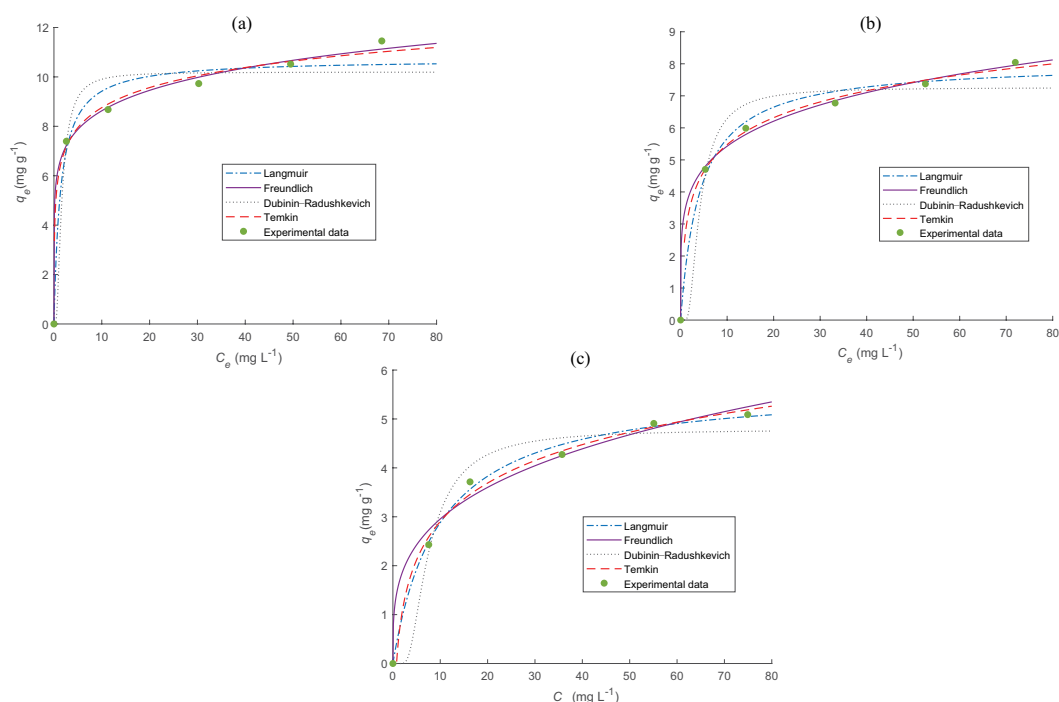


Fig. 7. Non-linear form of isotherm models for adsorption of Direct yellow 50 by GO-A at (a) 25°C, (b) 35°C, and (c) 45°C.

for the removal of Direct Yellow 50 from aqueous solutions. The average pore diameter and total pore volume were enhanced from 4.853 nm and 0.016 cm³/g to 42.879 nm and 0.133 cm³/g by modification process, respectively. The results showed that the Direct Yellow 50 followed non-linear Freundlich isotherm and Elovich

kinetic based on R^2 and error values. Moreover, the value of n suggests that the dye adsorption is favorable. The value of E_a (17.28 kJ/mol) confirmed a physical biosorption reaction of dye. Furthermore, an exothermic and a spontaneous nature for the adsorption process of the Direct Yellow 50 were displayed from thermodynamic

Table 5
Comparison of adsorption capacities for the removal of Direct Yellow 50 using various adsorbent materials

Adsorbent	Adsorption capacity (mg/g)	Ref.
GO-A	10.71	This study
PEI treated and immobilized biomass	15.7	[35]
Starch/acrylonitrile-amidoxime	2.8	[36]
Blank rice straw	0.6	[36]
Chemical treated rice straw	2.8	[36]
Lewatit VPOC 1064	19.4	[37]
Cotton fiber	28.57	[38]

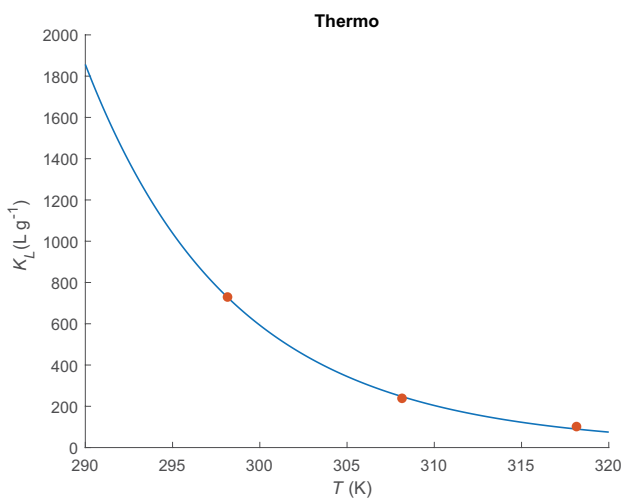


Fig. 8. The van't Hoff plot adsorption of Direct Yellow 50 by GO-A at different temperatures.

Table 6
Thermodynamic parameters for removal efficiency of Direct Yellow 50 onto GO-A adsorbent (90 min contact time, pH 7, and 1 g/L adsorbent, and 150 rpm agitation speed)

Temperature (K)	ΔG° (kJ/mol)	ΔH° (kJ/mol)	ΔS° (kJ/mol K)	R^2
298.15	-16.364			
308.15	-14.144	-82.554	-0.222	0.999
318.15	-11.924			

parameters. Based on the non-linear Langmuir isotherm, the maximum removal capacity for Direct Yellow 50 was 10.71, 8.03, and 5.71 mg/g for 25°C, 35°C, and 45°C temperatures, respectively. Finally, the adsorption characteristics of modified GO demonstrated that this adsorbent could be considered an effective one in the removal of Direct Yellow 50 from aqueous media.

Acknowledgements

The authors thank Dr. Armineh Azizi (Postdoctoral Research Fellow of Ryerson University) and Science and Research Branch, Islamic Azad University (SRBIAU) for their support.

References

- [1] M. Ghaedi, B. Sadeghian, A.A. Pebdani, R. Sahraei, A. Daneshfar, C. Duran, Kinetics, thermodynamics and equilibrium evaluation of direct yellow 12 removal by adsorption onto silver nanoparticles loaded activated carbon, *Chem. Eng. J.*, 187 (2012) 133–141.
- [2] A.A. El-Bindary, M.A. Hussien, M.A. Diab, A.M. Eessa, Adsorption of Acid Yellow 99 by polyacrylonitrile/activated carbon composite: kinetics, thermodynamics and isotherm studies, *J. Mol. Liq.*, 197 (2014) 236–242.
- [3] W. Hamza, N. Dammak, H.B. Hadjltaief, M. Eloussaief, M. Benzina, Sono-assisted adsorption of Cristal Violet dye onto Tunisian Smectite Clay: characterization, kinetics and adsorption isotherms, *Ecotoxicol. Environ. Saf.*, 163 (2018) 365–371.
- [4] A.A. Mir, A.A. Amooey, S. Ghasemi, Adsorption of direct yellow 12 from aqueous solutions by an iron oxide-gelatin nanoadsorbent; kinetic, isotherm and mechanism analysis, *J. Cleaner Prod.*, 170 (2018) 570–580.
- [5] A. Azizi, A. Torabian, E. Moniri, A.H. Hassani, H. Ahmad Panahi, Adsorption performance of modified graphene oxide nanoparticles for the removal of toluene, ethylbenzene, and xylenes from aqueous solution, *Desal. Water Treat.*, 57 (2016) 28806–28821.
- [6] M.C. Stanciu, M. Nichifor, Influence of dextran hydrogel characteristics on adsorption capacity for anionic dyes, *Carbohydr. Polym.*, 199 (2018) 75–83.
- [7] C. Puri, G. Sumana, Highly effective adsorption of crystal violet dye from contaminated water using graphene oxide intercalated montmorillonite nanocomposite, *Appl. Clay Sci.*, 166 (2018) 102–112.
- [8] J. Shen, S. Shahid, I. Amura, A. Sarihan, M. Tian, E.A.C. Emanuelsson, Enhanced adsorption of cationic and anionic dyes from aqueous solutions by polyacid doped polyaniline, *Synth. Met.*, 245 (2018) 151–159.
- [9] N.H. Othman, N.H. Alias, M.Z. Shahrudin, N.F. Abu Bakar, N.R. Nik Him, W.J. Lau, Adsorption kinetics of methylene blue dyes onto magnetic graphene oxide, *J. Environ. Chem. Eng.*, 6 (2018) 2803–2811.
- [10] Y. Qi, M. Yang, W. Xu, S. He, Y. Men, Natural polysaccharides-modified graphene oxide for adsorption of organic dyes from aqueous solutions, *J. Colloid Interface Sci.*, 486 (2017) 84–96.
- [11] Y. He, Y. Liu, T. Wu, J. Ma, X. Wang, Q. Gong, W. Kong, F. Xing, Y. Liu, J. Gao, An environmentally friendly method for the fabrication of reduced graphene oxide foam with a super oil absorption capacity, *J. Hazard. Mater.*, 260 (2013) 796–805.
- [12] E. Dadvar, R.R. Kalantary, H. Ahmad Panahi, M. Peyravi, Efficiency of polymeric membrane graphene oxide-TiO₂ for removal of azo dye, *J. Chem.*, 2017 (2017) 6217987 1–13, doi: 10.1155/2017/6217987.
- [13] A.A. Yakout, M.E. Mahmoud, Fabrication of magnetite-functionalized-graphene oxide and hexadecyltrimethyl ammonium bromide nanocomposite for efficient nanosorption of sunset yellow, *Mater. Sci. Eng. C*, 92 (2018) 287–296.

- [14] S. Chowdhury, R. Balasubramanian, Recent advances in the use of graphene-family nanoadsorbents for removal of toxic pollutants from wastewater, *Adv. Colloid Interface Sci.*, 204 (2014) 35–56.
- [15] W.S. Hummers, R.E. Offeman, Preparation of graphitic oxide, *J. Am. Chem. Soc.*, 80 (1958) 1339, doi: 10.1021/ja01539a017.
- [16] S. Mallakpour, S. Rashidmoghadam, Poly (vinyl alcohol)/ Vitamin C-multi walled carbon nanotubes composites and their applications for removal of methylene blue: advanced comparison between linear and nonlinear forms of adsorption isotherms and kinetics models, *Polymer*, 160 (2019) 115–125.
- [17] E.G. Sogut, N. Caliskan, Isotherm and kinetic studies of Pb(II) adsorption on raw and modified diatomite by using non-linear regression method, *Fresenius Environ. Bull.*, 26 (2017) 2721–2729.
- [18] P. Palanisamy, P. Sivakumar, Kinetic and isotherm studies of the adsorption of Acid Blue 92 using a low-cost non-conventional activated carbon, *Desalination*, 249 (2009) 388–397.
- [19] A.R. Tehrani-Bagha, H. Nikkar, N.M. Mahmoodi, M. Markazi, F.M. Menger, The sorption of cationic dyes onto kaolin: kinetic, isotherm and thermodynamic studies, *Desalination*, 266 (2011) 274–280.
- [20] A.A. Inyinbor, F.A. Adekola, G.A. Olatunji, Kinetics, isotherms and thermodynamic modeling of liquid phase adsorption of Rhodamine B dye onto *Raphia hookerie* fruit epicarp, *Water Resour. Ind.*, 15 (2016) 14–27.
- [21] Z. Zaheer, A.A. Aisha, E.S. Aazam, Adsorption of methyl red on biogenic Ag@Fe nanocomposite adsorbent: isotherms, kinetics and mechanisms, *J. Mol. Liq.*, 283 (2019) 287–298.
- [22] A. Azizi, M.R. Alavi Moghaddam, M. Arami, Comparison of three treated pulp and paper sludges as adsorbents for RB19 dye removal, *J. Residuals Sci. Technol.*, 8 (2011) 117–124.
- [23] H. Alrobei, M. Prashanth, C. Manjunatha, C.P. Kumar, C. Chitrabanu, P.D. Shivaramu, K.Y. Kumar, M. Raghu, Adsorption of anionic dye on eco-friendly synthesised reduced graphene oxide anchored with lanthanum aluminate: Isotherms, kinetics and statistical error analysis, *Ceram. Int.*, 47 (2021) 10322–10331.
- [24] A. Azizi, A. Torabian, E. Moniri, A.H. Hassani, H. Ahmad Panahi, Investigating the removal of ethylbenzene from aqueous solutions using modified graphene oxide: application of response surface methodology, *Int. J. Environ. Sci. Technol.*, 15 (2018) 2669–2678.
- [25] H. Yang, H. Li, J. Zhai, L. Sun, Y. Zhao, H. Yu, Magnetic Prussian blue/graphene oxide nanocomposites caged in calcium alginate microbeads for elimination of cesium ions from water and soil, *Chem. Eng. J.*, 246 (2014) 10–19.
- [26] V.K. Konaganti, R. Kota, S. Patil, G. Madras, Adsorption of anionic dyes on chitosan grafted poly(alkyl methacrylate), *Chem. Eng. J.*, 158 (2010) 393–401.
- [27] P. Sharma, B.K. Saikia, M.R. Das, Removal of methyl green dye molecule from aqueous system using reduced graphene oxide as an efficient adsorbent: kinetics, isotherm and thermodynamic parameters, *Colloids Surf., A*, 457 (2014) 125–133.
- [28] L.M. Tao, F. Niu, D. Zhang, T.M. Wang, Q.H. Wang, Amorphous covalent triazine frameworks for high performance room temperature ammonia gas sensing., *J. Chem.*, 38 (2014) 2774–2777.
- [29] K. Zhang, K.C. Kemp, V. Chandra, Homogeneous anchoring of TiO₂ nanoparticles on graphene sheets for waste water treatment, *Mater. Lett.*, 81 (2012) 127–130.
- [30] W. Konicki, M. Aleksandrak, E. Mijowska, Equilibrium, kinetic and thermodynamic studies on adsorption of cationic dyes from aqueous solutions using graphene oxide, *Chem. Eng. Res. Des.*, 123 (2017) 35–49.
- [31] W. Konicki, M. Aleksandrak, D. Moszyński, E. Mijowska, Adsorption of anionic azo-dyes from aqueous solutions onto graphene oxide: equilibrium, kinetic and thermodynamic studies, *J. Colloid Interface Sci.*, 496 (2017) 188–200.
- [32] K.B. Fontana, E.S. Chaves, J.D.S. Sanchez, E.R.L.R. Watanabe, J.M.T.A. Pietrobelli, G.G. Lenzi, Textile dye removal from aqueous solutions by malt bagasse: isotherm, kinetic and thermodynamic studies, *Ecotoxicol. Environ. Saf.*, 124 (2016) 329–336.
- [33] M. Ghaedi, B. Sadeghian, S.N. Kokhdan, A.A. Pebdani, R. Sahraei, A. Daneshfar, A. Mihandoost, Study of removal of Direct Yellow 12 by cadmium oxide nanowires loaded on activated carbon, *Mater. Sci. Eng. C*, 33 (2013) 2258–2265.
- [34] N.M. Mahmoodi, B. Hayati, M. Arami, C. Lan, Adsorption of textile dyes on Pine Cone from colored wastewater: kinetic, equilibrium and thermodynamic studies, *Desalination*, 268 (2011) 117–125.
- [35] S. Sadaf, H.N. Bhatti, S. Nausheen, M. Amin, Application of a novel lignocellulosic biomaterial for the removal of Direct Yellow 50 dye from aqueous solution: batch and column study, *J. Taiwan Inst. Chem. Eng.*, 47 (2015) 160–170.
- [36] S. Abdel-Aal, Y. Gad, A. Dessouki, Use of rice straw and radiation-modified maize starch/acrylonitrile in the treatment of wastewater, *J. Hazard. Mater.*, 129 (2006) 204–215.
- [37] M. Wawrzkiwicz, E. Polska-Adach, Z. Hubicki, Polycrylic and polystyrene functionalized resins for direct dye removal from textile effluents, *Sep. Sci. Technol.*, 55 (2020) 2122–2136.
- [38] L. Ismail, H. Sallam, S.A. Farha, A. Gamal, G. Mahmoud, Adsorption behaviour of direct yellow 50 onto cotton fiber: equilibrium, kinetic and thermodynamic profile, *Spectrochim. Acta, Part A*, 131 (2014) 657–666.
- [39] M.E. Mahmoud, G.M. Nabil, N.M. El-Mallah, H.I. Bassiouny, S. Kumar, T.M. Abdel-Fattah, Kinetics, isotherm, and thermodynamic studies of the adsorption of reactive red 195 A dye from water by modified Switchgrass Biochar adsorbent, *J. Ind. Eng. Chem.*, 37 (2016) 156–167.